Shape-specific activation of occipital cortex in an early blind echolocation expert

Stephen R. Arnott[1], Lore Thaler[2], Jennifer Milne[3], Daniel Kish[4], Melvyn A. Goodale[3]

[1]The Rotman Research Institute, Baycrest, 3560 Bathurst Street, Toronto, Ontario, Canada, M6A 2E1, [2]Department of Psychology, Durham University, Durham, UK [3]Department of Psychology, Western University, London, Ontario, Canada, N6A 5C2, [4]World Access for the Blind, Encino, California, Unites States of America, 91316

Running Title: Task-dependent echolocation activation

Corresponding Author:
Stephen R. Arnott
Rotman Research Institute
Baycrest Centre
Toronto, Ontario, Canada M6A 2E1
e-mail: *sarnott@research.baycrest.org*
phone: 1+ 416-785-2500 x2335

Abstract

We have previously reported that an early-blind echolocating individual (EB) showed robust occipital activation when he identified distant, silent objects based on echoes from his tongue clicks (Thaler, Arnott & Goodale, 2011). In the present study we investigated the extent to which echolocation activation in EB's occipital cortex reflected general echolocation processing per se versus feature-specific processing. In the first experiment, echolocation audio sessions were captured with in-ear microphones in an anechoic chamber or hallway alcove as EB produced tongue clicks in front of a concave or flat object covered in aluminum foil or a cotton towel. All eight echolocation sessions (2 shapes x 2 surface materials x 2 environments) were then randomly presented to him during a sparse-temporal scanning fMRI session. While fMRI contrasts of chamber versus alcove-recorded echolocation stimuli underscored the importance of auditory cortex for extracting echo information, main task comparisons demonstrated a prominent role of occipital cortex in shape-specific echo processing in a manner consistent with latent, multisensory cortical specialization. Specifically, relative to surface composition judgments, shape judgments elicited greater BOLD activity in ventrolateral occipital areas and bilateral occipital pole. A second echolocation experiment involving shape judgments of objects located 20 degrees to the left or right of straight ahead activated more rostral areas of EB's calcarine cortex relative to location judgments of those same objects and, as we previously reported, such calcarine activity was largest when the object was located in contralateral hemispace. Interestingly, other echolocating experts (i.e., a congenitally blind individual in Experiment 1, and a late blind individual in Experiment 2) did not show the same pattern of feature-specific echo-processing

calcarine activity as EB, suggesting the possible significance of early visual experience and early echolocation training. Together, our findings indicate that the echolocation activation in EB's occipital cortex is feature-specific, and that these object representations appear to be organized in a topographic manner.

Keywords: auditory; blind; echolocation; fMRI; occipital cortex; retinotopy

It is now well recognized that humans, like dolphins and bats, can actively produce sounds in order to acquire echo information that enables them to localize and identify silent objects in their surrounding environment (Schenkman & Nilsson, 2010; Stoffregen & Pittenger, 1995; Teng, Puri, & Whitney, 2012; Teng & Whitney, 2011; Thaler, Arnott, & Goodale, 2011). We have recently reported the first functional brain imaging investigation of active echolocation in humans, showing that the calcarine cortices of an early blind (EB) and a late blind (LB) echolocation expert were activated when they identified otherwise silent objects from echolocation audio recordings (Thaler et al., 2011). Specifically, when lying in a magnetic resonance imaging (MRI) machine and listening to binaural in-ear audio recordings of their pre-recorded echolocation mouth clicks sessions that included echo information, both participants were not only able to identify the silent objects present in the recordings, but their corresponding blood oxygen-level dependent (BOLD) activity was found to increase in auditory and occipital cortices. Most impressively, when this brain activity was contrasted with that related to listening to the same sounds but with the very faint echoes removed, activity in occipital but not auditory cortex remained. The results indicated that the processing of the echo information was being carried out in occipital cortex.

In the present study we wished to further explore EB's echo-related brain activity by examining the functional MRI (fMRI) responses associated with extracting different object features from the same echolocation recordings. For example, to what extent does the brain activity differ between different types of object feature processing, e.g. shape, location or material? Moreover, if such feature-specific activations are found, do they

occur in cortical regions normally associated with similar types of feature processing within the auditory and/or visual modality?

In sighted individuals, visual form perception is typically associated with increased haemodynamic activity in the inferotemporal and occipito-temporal brain regions (e.g., the lateral occipital complex (LOC), Cant, Arnott, & Goodale, 2009; Grill-Spector, Kourtzi, & Kanwisher, 2001; Haxby et al., 2001; Malach et al., 1995), as is tactile form perception in sighted (Amedi, Malach, Hendler, Peled, & Zohary, 2001; James et al., 2002) and non-sighted individuals (Burton, Snyder, Diamond, & Raichle, 2002; Ptito et al., 2012). Owing to the fact that shape perception tends not to be as conspicuous from sound alone, evidence in favour of auditory-induced form activation of these areas is more equivocal. For example, while some studies investigating LOC activation in response to auditory stimuli have not supported an association (Amedi, Jacobson, Hendler, Malach, & Zohary, 2002), more recent studies in both blind and sighted individuals have, albeit often not without involving extensive auditory-shape training prior to functional imaging (Amedi et al., 2007; James, Stevenson, Kim, Vanderklok, & James, 2011; Kim & Zatorre, 2011; Lewis, Brefczynski, Phinney, Janik, & DeYoe, 2005; Ptito et al., 2012).

Brain regions involved in object localization on the other hand are more clear cut, with visual localization tasks activating regions of the occipital cortex, precuneus and posterior parietal lobe (Ungerleider, Courtney, & Haxby, 1998), and auditory localization tasks predominately activating the inferior parietal lobule as well as the posterior superior temporal sulcus, and superior frontal sulcus (frontal eye fields, Arnott, Binns, Grady, & Alain, 2004). In the blind, sound localization has additionally been found to activate

dorsal regions of the occipital cortex (Collignon, Voss, Lassonde, & Lepore, 2009; Weeks et al., 2000). With respect to the processing of an object's surface composition (e.g., whether an object is soft or hard, wood or rock), several visual studies have noted the importance of medial ventral brain areas including the collateral sulcus, inferior occipital gyrus, and posterior parahippocampal area (Cant et al., 2009; Cant & Goodale, 2011; Cavina-Pratesi, Kentridge, Heywood, & Milner, 2010). A proximal region in the posterior parahippocampus has also been found to respond to aurally-conveyed object surface composition (Arnott, Cant, Dutton, & Goodale, 2008).

A secondary question that the topic of feature-specific activation in the blind raises relates to the broader issue in sensory substitution literature concerning how the occipital lobe is colonized by non-visual sensory input, once it is deprived of visual input as occurs in the blind (c.f., Collignon, Vandewalle et al., 2011). Converging evidence indicates that the age of onset of visual deprivation affects the degree of functional as well as structural brain reorganization that occurs within occipital cortex, with the largest amount of reorganization occurring when sight loss coincides with sensitive periods of neurodevelopment (for a review, see Noppeney, 2007). EB's visual loss at age one year old as well as his active use of echolocation shortly thereafter, certainly coincides with such a sensitive period as the synaptic density in his striate cortex, having reached its apex only months before, would have just started its decade-long process of synaptic pruning (Huttenlocher & de Courten, 1987). It is therefore possible that the functional patterns of echolocation activity within striate cortex may differ depending on when an echolocator lost his or her sight and began to actively echolocate.

To investigate these questions, we present results from two fMRI echolocation experiments in which our echolocating expert, EB performed object feature judgments. In Experiment 1, mouth click 'echolocation' recordings made in front of silent objects of different shapes (flat disc or concave) and covered in different materials (aluminum foil or cotton towel) were presented to EB while he made shape or material judgments of the 'silent' objects based on the echo information in those recordings. In Experiment 2, echolocation recordings made in front of a flat or concave object located 20° to the left or right of straight ahead were presented to EB while he made shape or location judgments. We were particularly interested in determining whether extracting different object features from the exactly the same auditory (i.e., echo) input would activate similar areas of cortex, especially in the occipital lobe, and how this would replicate across different experiments. Finally, in order to get a sense of the uniqueness of EB's functional results with respect to his case history, we present results from two additional blind echolocating experts (CB in Experiment 1 and LB in Experiment 2) who differed from EB in terms of age-of-onset of blindness (i.e., congenital blindness and late blindness) and echolocation histories.

Based on our previous work with EB (Thaler et al., 2011), as well as other work on auditory processing in the blind (c.f., Amedi et al., 2007), it was expected that echo-specific shape recognition in EB would invoke activity in the ventrolateral occipital areas such as the fusiform gyrus and area LOC. Importantly, this type of activity was expected to be enhanced relative to when EB listened to exactly the same sounds, but was required to extract another object feature such as material properties (Experiment 1) or location properties (Experiment 2), that could only be acquired through the echo processing of the

mouth clicks. Moreover, given that EB lost his sight at critical period in his visual development, we were interested to see how activation in his striate cortex would compare to those of a congenitally blind and late blind echolocator.

3. Material and Methods

All testing procedures were approved by the ethics board at Western University, and the participants gave informed consent prior to testing.

3.1 Participants

Participant EB was a 45 year-old right-handed male who had his first eye removed at age 7-months followed by his second eye at age 13-months due to retinoblastoma. EB reported normal hearing, and this was confirmed by audiological testing results (Thaler et al., 2011). EB has been using echolocation since "as long as (he) can remember", and continues to use it on a daily basis to navigate as well as to perceive and interact with objects in the world. He produces his echolocation sounds using tongue clicks generated by a quick withdrawal of the tongue tip from the front palate (i.e., oral click, Rojas, Hermosilla, Montero, & Espi, 2009). Prior amplitude measurements (Larson-Davis System 824) of EB's clicks registered intensities between 71 and 74 dB SPL at the ear, dropping to approximately 53.6 and 49.0 dB SPL at distances of 1m and 2m respectively.

Control participants CB (Experiment 1) and LB (Experiment 2) were blind individuals who also echolocate on a daily basis, but who did not start (actively or consciously) doing so until later in life. CB was a 44 year-old right-handed male who lost his vision at birth due to retinopathy of prematurity. He did not begin to actively echolocate until approximately age 40 years-old. LB was a 27 year-old right-handed

male who lost his vision at age 14 years and who began echolocating approximately three years after that. At the time of testing, all participants were acting as Orientation and Mobility coaches, teaching the technique of active echolocation to others.

3.2 Echolocation objects

Experiment 1: Four objects were used for generating echolocation stimuli. Each was constructed of wire mesh (wire gauge 0.8 mm; spacing of 4.0 mm^2). Two of the objects were disc-shaped (30 cm diameter), while the remaining two were bowl-shaped (30 cm in diameter, 12 cm depth). One of each unique-shaped object was covered with non-smooth (i.e., crinkled) 'heavy-duty' household aluminum foil material (~0.024 mm thickness), while the remaining two objects were covered with a thin cotton, towel-material.

Experiment 2: Two echolocation objects were used. The first was a rigid concave-shaped plastic object approximately 30 cm diameter and 15 cm in depth oriented with the concavity facing the listener. The second was a 12 cm painted wooden cube positioned such that one side was oriented squarely at the listener. Objects were located 40 cm from the seated listener, and mounted on a 0.5 cm diameter telescopic steel pole at a height even with that of the participant's mouth (i.e., approximately 1.3 m above the floor) and at an azimuth position of either 20° to the left or right of straight ahead.

3.3 Experimental stimuli and recording procedure

Experiment 1: Similar to our previous study (Thaler et al., 2011), audio stimuli were created by recording each participant's echolocation clicks (including the subsequent echoes) as he stood directly in front of the echolocation objects at a distance of 30 cm from his face (i.e., subtending a visual angle of 53° directly in front of the observer), with his head held stationary and oriented straight ahead. Disc-shaped objects were arranged

so that the flat surface was oriented directly at the participant. Bowl-shaped objects were arranged with the concave surface facing the echolocator. Each object was mounted on a 0.5 cm diameter pole that was vertically adjusted to ear-level. For each of the four objects, the participant emitted three 10-s volleys of echolocation calls. The rate of clicking was self-paced with the inter-click interval tending to range between 0.4-1.0-s.

The audio from these clicking sessions was recorded via in-ear binaural omni-directional microphones (Sound Professionals-TFB-2; 'flat' frequency range 20 – 20,000 Hz) attached to a portable Edirol R-09 digital wave recorder (16-bit, stereo, 44.1 kHz sampling rate). Microphones were placed directly at the opening of EB's left and right auditory canals and held in place by a soft rubber 'horn-shaped' housing that conformed to the shape of the concha. In addition, 'silent background' recordings of approximately 20-s was made as each participant stood quietly in position without emitting any clicks.

The clicking sessions (as well as the silent background conditions) were recorded at two acoustically distinct locations at the National Centre for Audiology in London, Ontario, Canada. The first location (*chamber*) was in a Beltone Anechoic Chamber measuring 5.5 m high x 7.0 m wide x 3.7 m deep, and equipped with a 125 Hz cut-off wedge system on the walls and ceiling. The chamber floor was covered in foam baffles. The entire recording session was then repeated later on in the day in a second location (*alcove*) that consisted of a small alcove off of a hallway outside of the chamber measuring 2.7 m high x 1.4 m wide x 2.0 m deep. The walls of the alcove were composed of drywall board, the ceiling of fibreglass ceiling panels, and the concrete floor had a vinyl surface.

Experiment 2: With the exception that the stimuli were located 40 cm away from the seated listener, were offset from straight ahead by 20° to the left or right, and no foam baffles had been placed on the floor, the recording parameters of Experiment 2 were the same as those of the anechoic chamber in Experiment 1.

3.4 Audio editing and presentation

Experiment 1: Sound editing was performed with Adobe Audition software (version 1.5; Adobe Systems, San Jose, CA, USA). As a result of offline microphone calibration measurements, the recorded signal from the right channel was amplified 0.78 dB SPL in order to achieve a between-channel correspondence of 0.01 dB SPL (±0.29 dB Standard Deviation (SD)). Next, each participant's 24 recorded click volleys (3 samples x 4 objects x 2 locations) were clipped to durations ranging between 5 and 10-s. Accordingly, 24 unique echolocation audio clips were created for each participant. In addition, 'control' sounds were created for the Baseline condition from a representative subset of each participant's echolocation calls in a manner similar to our earlier study (Thaler et al., 2011). Specifically, for a given echolocation clip, the click waveforms (i.e., the ~10-ms of audio following the onset of each click) were extracted and then overlaid on the corresponding 'silent' background recording (i.e., on the silent recording made in either the chamber or the alcove). As a result, the control stimuli were virtually identical to the experimental stimuli in terms of overall acoustic energy and timing, with the exception of the missing click echoes. Amplitude statistical measurements of the recorded echolocation stimuli were carried out on each waveform using Adobe Audition (version 1.5). Minimum, maximum, average and total root mean square (RMS) power estimates were obtained using a 50-ms window, with the dB level corresponding to a FS

(full-scale) square wave in which the peak amplitude level was set to 0 dB, using every sample in a 16-bit range.

MRI audio stimuli were delivered to the listener using a Sensimetrics MRI-compatible insert earphone system (model S14). To compensate for the system's reliable, yet non-flat, frequency response of up to 10 kHz, frequency response equalization (0 – 10 kHz) was performed on all experimental sound files using the manufacturer's equalization filters (Sensimetrics, Malden, MA, USA). The insert earphone tips were encased in disposable foam tips providing a 20-40 dB attenuation level (information provided by the manufacturer). Further sound attenuation was attained by placing foam inserts between the head rest and the listener's ears. To minimize background noise, the MRI bore's circulatory air fan was turned off during experimental runs. Experimental stimuli were presented using Matlab software (R14, The Mathworks). Functional MRI data were analyzed using Brain Voyager QX (v.2.3, Brain Innovation, Maastricht, The Netherlands).

Experiment 2: Audio stimuli were edited and presented in a similar way, with the exception that no Baseline "control" sounds were created (i.e., silence was the baseline condition). The reason for this as well as other methodological inconsistencies between the experimental designs of Experiments 1 and 2 stem from the fact that the latter had originally been designed as part of a separate series of experiments (Thaler et al., 2011).

3.5. fMRI data acquisition

Imaging was performed at the Robarts Research Institute (London, Ontario, Canada) on a 3-Tesla, whole-body MRI system (Magnetom Tim Trio; Siemens, Erlangen, Germany) using a 32-channel head coil. For the functional scans, 38

contiguous axial slices covering the whole brain were acquired in ascending interleaved order using a single-shot gradient T2*-weighted, echo-planar pulse sequence in combination with a sparse-sampling design (Hall et al., 1999). TR = 14s (12-s silent gap + 2-s slice acquisition); TE = 30-ms; flip angle = 78°; FOV = 211mm; 3.3 mm x 3.3 mm x 3.5 mm; 64 x 64 effective acquisition matrix. Each run consisted of 26 volumes. All functional scans were aligned to a high-resolution (1 mm x 1mm x 1mm), single-shot T1-weighted anatomical MRI image obtained with an optimized sequence (MPRAGE).

3.5.1 Stimulus Presentation

Experiment 1: For a schematic illustration, refer to Figure 1. Each run contained a pseudo-random presentation of baseline and experimental trials. All trials began with a pre-recorded spoken instruction indicating whether the trial was a baseline (i.e., "control"), or an experimental trial (i.e., "shape", "material", or "place"). Experimental trial instructions informed the listener what type of attribute he was to judge from the subsequent click volley. Total time including the brief silent gap that followed the instruction was 1-s. Next, a 10-s click volley was presented with all clicks in that volley being made to the same object. Audio clips that were less than 10-s were looped until the 10-s had transpired. Following the click volley, a 200-ms 1000Hz tone (i.e., response cue) instructed the participant to indicate his response with a button press (right index finger response = flat shape, aluminum foil material, or alcove place; right middle finger response button = concave shape, towel material, or chamber place). For control trials, the participant was asked to press either response button upon hearing the tone. Functional scans started 12-s after the onset of the run, and lasted 2-s. The next trial started after scanning had ended.

Insert Figure 1 about here

Trials were counterbalanced such that a baseline trial always preceded three experimental trials (i.e., one 'shape', one 'material' and one 'place' trial, randomly ordered). Each run began and ended with a baseline trial. The total number of trials in each run was 25 (6 shape, 6 material, 6 place and 7 baseline) and each run lasted 25 x 14-s. The order of these 25 trials was maintained for all runs. EB and CB each performed a total of 8 runs across two sessions (6 runs in the first session, and 2 in the second session).

A pos-hoc behavioural control experiment was also run on 3 sighted individuals (age 36, 38, and 33 years old) to test how non-echolocating listeners would perform on the Place task. Two examples of each of the eight conditions (2 shapes x 2 materials x 2 places) were low-pass filtered at 10kHz and then presented to the participants from a computer laptop using Sennheiser (HD280) headphones. After being given several examples of each type of shape, material and place differences, participants listened to the group of 16 stimuli three times, making Place, Shape, and Material judgments, respectively.

Experiment 2: Refer to bottom panel of Figure 1. Stimulus presentation was the same as Experiment 1, with the exception that the pre-recorded audio instruction informed the participant to attend to either the "shape" or "location" feature. Responses were made with the right hand with the index finger indicating 'concave' or 'left' and the middle finger indicating 'flat' or 'right'. Unlike Experiment 1, the Baseline task was not an

echoless control sound, but rather a silent listening condition where no button press occurred. Trials were counterbalanced such that a silent trial always preceded two experimental trials, with the experimental trials occurring in alternating order (i.e. shape-location followed location-shape and vice versa). Each run began and ended with a silent baseline trial. The total number of trials in each run was 25 (8 shape, 8 location and 9 silent) and each run lasted 25 x 14-s. EB and LB each performed 5 runs.

3.6 fMRI data analysis

3.6.1. Pre-processing and co-registration

All MRI data were processed and analyzed with Brain Voyager QX, Version 2.3.1. (Brain Innovation, Maastricht, The Netherlands). For each echolocation run, the dummy volume was discarded from functional data analysis, but used for functional-to-anatomical co-registration. Each run was subjected to Slice Scan Time Correction (Tri-linear sinc), temporal High-Pass Filtering (cut-off at 2 sines/cosines) and 3D Motion correction (Tri-linear sinc). For quality assessment the motion parameters estimated for within-run motion for each run were inspected to ensure that they did not exceed 1° rotation and 1 mm translation within any given run. To align the functional data across runs within a session, the 3D motion correction function was used to align each volume within a run to the functional volume closest to the anatomical scan from the same session. With respect to Experiment 1, functional data from the session with the most runs (i.e., session 1) was transformed into standard stereotactic space (Talairach & Tournoux, 1988). To align the two functional runs from the second experimental session, the AC-PC aligned isometric voxel anatomical image from each participant's session 2 was co-registered with that of the respective participant's session 1 using the "Initial

Alignment" function followed by a "Gradient-based fine alignment" with "rigid" alignment functions. The anatomical image was then transformed into stereotactic space. These same transformation files were then applied to session 2's pre-processed functional runs. Functional data in Experiment 2 were pre-processed and co-registered in the same manner as Experiment 1.

3.6.2.1. Experiment 1: Voxelwise analysis

To obtain activity related to echo processing as compared to the "Control" -sound Baseline, a fixed-effect GLM was applied with the stick-predictors "Shape", "Material", and "Place" to the z-transformed time courses of runs. To determine where BOLD activity during echolocation trials exceeded that during the baseline "Control" trials, voxels where the beta value of the 'Echo' predictor was significantly larger than zero were isolated. The significance threshold for evaluation of results in volume space was set to 0.05 in order to remove obvious false positives (e.g., activations outside of the brain) while still showing positive activation. Furthermore, a minimum activation cluster size of 430 voxels was also implemented using AFNI's (Cox, 1996) AlphaSim-based 3dClustSim program, in order to ensure with 95% probability that such thresholded activations were not due to chance. In recognition of the fact that this whole-brain voxel-wise approach and cluster thresholding criteria may have overlooked small but significant areas of brain activation, 'near-significantly-sized' clusters of activity of 225 voxels or greater.are also listed in the Tables and/or Figures.

As part of a post-hoc examination of the effect of different echolocation recording environments (i.e., in the anechoic chamber or in the hallway alcove), a similar fixed-effect GLM was applied using the control-sound recorded in the chamber as the Baseline

(i.e., “chamber Control”). For this analysis, stick-predictors of “alcove Control”, “chamber Shape”, “alcove Shape”, “chamber Material”, “alcove Material”, “chamber Place” and “alcove Place” were created.

3.6.2.2. Experiment 2: Voxelwise analysis

As in Experiment 1, a fixed-effect GLM was applied but using stick-predictors of “Shape” and “Location” to the z-transformed time courses of runs. To determine where BOLD activity during echolocation trials exceeded that during the silent baseline trials, voxels where the beta value of the task predictor was significantly larger than zero were isolated. Due to the use of a silent baseline condition, activation clusters were generally larger in Experiment 2 than in Experiment 1, so the significance threshold for evaluation of results in volume space was set to 0.01 (rather than 0.05) with a 95% 3dClustSim reliability measure being achieved when the activation cluster size was at least 191 voxels. As with Experiment 1, ‘near-significant’ sized clusters of activity (i.e., 110 voxels or more) a re also listed in the Tables and/or Figures.

3.6.2.3. Experiment 2: ROI analysis

The ROI analysis of the fMRI results from Experiment 2, previously reported elsewhere (see Thaler et al., 2011), adopted an independent functional (i.e., an independent fMRI experiment involving echolocation processing of left and right objects: refer to Figure 4 of Thaler et al., 2011) and structural (i.e., voxels had to be proximal to the calcarine sulcus and within calcarine cortex) approach to define two echolocation ROIs in each participant: one in the left and one in the right calcarine cortex. This approach resulted in left and right ROIs of 919 and 2569 voxels, respectively for EB, and 88 and 128 for LB. The beta-values associated with Experiment 2’s echo judgments (i.e., Shape and

Location) of objects located to the left or right side of space were extracted separately from the voxels in each ROI and then statistically compared to one another using the number of trial observations as the degrees of freedom.

4. Results

4.1. Experiment 1: Shape, Material, Place (SMP)

4.1.1 Behavioural. As anticipated, the Place (P) task proved trivial for both echolocators with each performing at 100% accuracy. That the ability to perform well on the Place task was independent of the listener's ability to echolocate was supported by the fact that three sighted, non-echolocating individuals also performed with 100% accuracy on the Place control task, whereas their mean performance on the Material (M) and Shape (S) tasks were 52.1% (0.04 SD) and 54.2% (0.07 SD), respectively. The actual 'echo' tasks, noted by EB to be comparatively more difficult, were found to have accuracy rates of 58.3% and 91.7% for the Shape (S) and Material (M) trials, respectively. CB performed with accuracy rates of 62.5% and 54.2% on the S and M trials, respectively.

Although EB's performance on the Shape task was not comparatively different from chance ($t = 1.16$, $p > 0.1$), further analyses revealed that his echo performance was affected by the recording environment (i.e., in the chamber or the alcove). Indeed, collapsing across S and M tasks, it was found that EB performed significantly better on chamber compared to alcove trials ($t = 2.56$, $p < 0.05$). In terms of S-trials only, EB's chamber sound performance rose to 70.5% (12/17) which approached above chance levels (i.e., $t = 1.81$, $p = 0.09$, two-tailed test), but fell to 51.6% when assessing only the alcove recordings (n.b., in the behavioural control study, the sighted control participants'

mean performance was 42.6% and 58.3% for the chamber and alcove recordings, respectively, neither of which were significantly different from the chance score of 50%; both $p > 0.1$). EB's M-trial performance also benefited from chamber stimuli where he performed with perfect accuracy on chamber trials, but only 83.3% accuracy on alcove trials. These two scores were statistically different from one another ($t = 2.05$, $p < 0.05$). Sighted control participants scored 50.0% and 54.2% on Material chamber and alcove judgments, respectively. Because of the general trend effect of 'recording location' on EB's echo performance, subsequent data tables displaying fMRI activation during the Shape and Material conditions also display the corresponding fMRI signal values associated with the alcove and chamber recordings separately, in order to gauge the effect of task difficulty on a given brain region.

Neither CB's S nor his M accuracy scores differed from chance ($t = 1.77$ and $t = 0.57$, respectively), and he did not perform significantly better on one type of recording than the other (i.e., chamber versus alcove). CB's chS and alS accuracy scores were 59.1% and 65.4%, respectively; neither of which were different from chance ($t = 0.85$ and 1.62, respectively) nor from one another ($t = 0.44$). CB's chM and alM accuracy scores were 72.0% and 34.8%, respectively, with the chamber ($t = 2.40$, $p < 0.05$) but not the alcove ($t = -1.50$, *n.s.*) recordings being performed significantly above chance levels. chM and alM accuracy were significantly different from one another ($t = 2.73$, $p < 0.01$).

4.1.2 RMS analysis of waveform amplitudes

EB: Across all of the S-trials, alcove-recorded waveforms from EB were found to have a larger Average RMS power value than chamber recordings [alcove = -42.18 dB (1.38 SD), chamber = –49.19 dB (2.82 SD); $t = 11.61$, $p < 0.001$]. The same pattern was found

in the Material trials, with alcove recordings showing a greater Average RMS power level than chamber recordings [alcove = -42.28 dB (1.38 SD), chamber = -49.68 dB (2.33 SD); $t = 13.41$, $p < 0.001$]. This difference in overall background noise level also translated into a better signal-to-noise ratio for the chamber versus alcove recordings. A comparison of the Minimum and Maximum RMS power levels across the different recording locations demonstrated that chamber recordings had a lower mean Minimum RMS value than the alcove recordings [Shape task: alcove = -51.71 dB (5.11 SD), chamber = -60.50 dB (7.82 SD), $t = 4.70$, $p < 0.001$; Material task: alcove = -51.66 dB (4.81 SD), chamber = -62.66 dB (6.74 SD), $t = 6.51$, $p < 0.001$], but that the alcove click recordings had a higher mean Maximum RMS value than the chamber recordings [Shape task: alcove = -35.63 dB (0.66 SD), chamber = -39.37 dB (1.76 SD), $t = 10.61$, $p < 0.001$; Material task: alcove = -35.65 dB (0.63 SD), chamber = -38.95 dB (1.59 SD), $t = 9.43$, $p < 0.001$].

CB: For CB, alcove-recorded trials had a larger average RMS value than chamber-recorded trials, both during S-trials [alcove = -37.03 dB (0.66 SD), chamber = -40.59 dB (0.52 SD); $t = 20.44$, $p < 0.001$] and M-trials [alcove = -37.10 dB (0.59 SD), chamber = -40.38 dB (0.55 SD); $t = 19.92$, $p < 0.001$]. Unlike with EB, the comparison of Minimum and Maximum RMS power levels across the two recording locations revealed that the alcove recordings made of CB's clicks had a 'quieter' minimum RMS level than the chamber recordings [Shape task: alcove = -46.54 dB (0.35 SD), chamber = -45.80 dB (0.85 SD); $t = -4.10$, $p < 0.001$; Material task: alcove -46.41 dB (0.48 SD), chamber -45.77 dB (0.80 SD); $t = -3.32$, $p < 0.005$]. As with EB, the alcove recordings had a higher Maximum RMS value than chamber recordings [Shape: alcove = -22.55 dB (1.73

SD), chamber = -24.73 dB (2.33 SD); $t = 3.70$, $p < 0.001$. Material: alcove = -22.50 dB (1.88 SD), chamber = -24.51 dB (1.97 SD); $t = 3.61$, $p < 0.001$].

4.1.3 fMRI analysis

Echo-specific activity

S & M > P (balanced) ∩ S & M > Baseline (Echoless clicks). Relative to the Place task and the control sounds of the Baseline task, the two echo-specific tasks (i.e., Shape and Material) were associated with increased BOLD signals in the right angular gyrus, right inferior temporal gyrus, left Brodmann Area (BA) 9 in the frontal lobe as well as the anterior cingulate in EB (Figure 2, Table S1). In addition, activity in the left angular gyrus, posterior cingulate, bilateral posterior hippocampus (especially in the right hemisphere), and regions of the cerebellum were also observed. Near-significant sized voxel clusters were also noted in the left posterior middle temporal gyrus (LOC).

Insert Figure 2 about here

CB also showed similar activity in the right angular gyrus, left inferior frontal gyrus and anterior cingulate. Near-significant activity was also registered in CB's right anterior inferior temporal gyrus, right inferior frontal gyrus, left medial frontal gyrus, left middle temporal gyrus, and right LOC (209 voxels). No activity, however, was observed in the hippocampal region, even at reduced threshold levels. See Figure S1 and Table S2.

Feature-specific echo activity

S > M:

EB: Compared to the Material task, significantly greater Shape task BOLD activity was found in bilateral regions of the inferior occipital gyrus (BA17), fusiform gyrus, posterior MTG, posterior cingulate, and precuneus (See Figure 3 and Table S3). Greater Shape activity was also found in the right caudate, left anterior cingulate, left middle frontal gyrus, left putamen, and in regions of the cerebellum. Near-significant sized voxel clusters were also noted in the right SPL, right precuneus, and right parahippocampal gyrus. Breaking the Shape trials down according to the environment that they were recorded in (i.e., chS versus alS, bottom plots of Figure 3, Table S3) demonstrated that in all of these regions of interest, the mean BOLD signal level was equal if not larger during EB's chamber trials compared to his alcove trials. A formal comparison of chS and alS trials (Table S4b) confirmed the greater chamber compared to alcove activation in left fusiform and occipital pole.

Insert Figure 3 about here

As a further test of the validity of these shape processing regions, a conjunction contrast of S > M ∩ S > Baseline (echoless control sounds) for EB was also carried out. Of the aforementioned S > M regions, only the left occipital pole (IOG), bilateral (stronger in the left hemisphere) posterior middle temporal gyri/precuneus (BA39/19), posterior cingulate and cerebellum survived the statistical thresholds (see orange overlap activity in Figure 3, and boldface type brain areas in Table S3).

CB: Figure S2 and Table S5 show the results for the S > M as well as the more stringent S > M ∩ S > Baseline (echoless control sounds) contrast. CB showed S > M activity in

the right inferior and medial frontal gyri, left middle frontal gyrus, left insula, right cerebellum extending into the lingual and fusiform gyri. Although his activation of occipital cortex was not nearly as extensive as EB's, CB did show S > M activation in the superior occipital gyrus and lingual gyrus in the left hemisphere, the left cerebellum, and areas of the brainstem. Of these, only the brainstem response was significantly activated in the conjunction contrast of S > M ∩ S > Baseline (i.e., boldface type brain areas in Table S5).

M > S:

EB. Relative to the Shape trials, greater BOLD activity for the Material trials was found in the right supramarginal gyrus, as well as in several frontal regions including bilateral SFG, and the left medial frontal gyrus. Near-significant sized voxel clusters were noted in the left anterior STG and middle frontal gyrus (Figure 3 and Table S3). None of these areas was significantly active when the conjunction contrast of M > S ∩ M > Baseline was carried out, nor were those areas significantly affected by whether the sound had been recorded in the chamber or the alcove (see Table S4c).

CB. Greater Material versus Shape activity was observed in the precuneus, left SPL, and L anterior parahippocampus. Near-significant sized voxel clusters were also observed in the left and right parahippocampus as well as left and right cerebellum (see Table S5). As with EB, no areas for CB were found to be significantly active with the conjunction contrast of M > S ∩ M > Baseline.

P > S ∩ P > M ∩ P > Baseline (Echoless clicks).

EB. Relative to the Shape and Material trials as well as the echoless-click Baseline trials, EB's Place trials were associated with increased activity along the length of the right

calcarine sulcus (see inset of Figure 2, Table S6a). Within each of these regions of activation, the average beta weight voxel values during the Shape and Material trials were significantly below baseline (i.e., echoless click sound) levels (Table S6a). A similar Place-selective activation was also found in the right precuneus.

CB. Like EB, the Place-specific contrast for CB also showed significant activity in the right calcarine sulcus and cuneus (see inset of Figure S1 and Table S6b). In addition, areas within the right and left middle frontal gyri were also activated during the Place task.

Chamber versus Alcove Echo processing (chS & chM vs. alS & alM). An overall contrast of echo processing (i.e., those tasks that could only be accomplished by interpreting the click echoes: S and M) according to the different locations in which the recordings were taken (i.e., anechoic chamber (ch) or hallway alcove (al)), revealed the following for EB (Figure 4a; Table S4). First, it was only ever the case that significantly greater activity was found for chamber sounds compared to the alcove, and not the reverse. These activations were located bilaterally along Heschl's gyrus and in auditory cortex, as well as scattered throughout regions of 'visual' cortex including the left lingual gyrus, and cuneus. Near-significant sized voxel areas of activity were also observed in the left middle occipital gyrus, right precuneus, and left angular gyrus.

Insert Figure 4 about here

A similar pattern was observed for CB in the Shape and Material echo tasks, with all activity being greater during chamber compared to alcove recordings. The areas

of activation included the right auditory cortex, left auditory cortex/insula, as well as bilateral occipital regions including the middle occipital gyri and lingual gyri, the right cuneus, left inferior occipital gyrus, and left precentral gyrus (Figure S3, and Table S7).

chS vs. alS. A comparison of EB's chamber and alcove trials during only the S task revealed significantly greater chamber sound activation in bilateral Heschl's gyrus, as well as near-significant sized cluster in the left anterior STG (Figure 4b, Table S4b). Within occipital areas, the left cuneus was also more significantly activated by the chamber sounds. Regions within the left middle occipital gyrus, fusiform gyrus and insula showed sub-voxel threshold activity. We also compared the chS and the alS beta-weights within the ROIs obtained from the S > M comparison (above). Once again, none of the ROIs had a mean alcove Shape beta-weight value that was greater than the corresponding mean chamber Shape beta-weight, although the opposite pattern was observed for some areas including the posterior cingulate, the left precuneus/MTG and the left fusiform region. With respect to CB, the only region that showed differential activity was the chS > alS region in the right Middle Occipital Gyrus (see Figure S3b and Supplemental Table S7b).

chM vs. alM. A similar comparison among Material trials revealed only one significant area of chamber > alcove activation and this was located in the medial aspect of left Heschl's gyrus (Figure 4b, Table S4c). On the other hand, CB showed chM > alM activity in several posterior areas including bilateral cuneus, left calcarine, and left middle and superior occipital gyri (see Figure S3b and Table S7c).

chP vs. alP. The contrast of chamber and alcove recordings within the Place task did not reveal any significant (or near-significant) areas of activity for either echolocator (Tables S4d and S7d).

alControl vs. Baseline (chControl). A comparison of the alcove Control condition with that of the (Baseline) chamber Control condition revealed only alcove > chamber activity for EB. None of these regions were located in or around the STG, but were instead confined to regions of the precuneus and SPL bilaterally, as well as near-significant sized regions of left lingual gyrus, paracentral lobule,and postcentral gyrus (Table S4e). The same contrast for CB revealed a similar but more extensive pattern of alcove > chamber activity involving bilateral parietal and occipital regions, dorsolateral frontal cortex as well as auditory cortex (see Table S7e). Only two regions, the right angular gyrus and left medial frontal gyrus, showed greater chamber versus alcove activity.

4.2. Experiment 2: SL

4.2.1 Behavioural. A technical error precluded the behavioural responses from being recorded during the Shape-Location task of Experiment 2. Nevertheless, when the participants re-performed the same experiment a few hours later outside of the MRI room, but using the same MRI audio system, EB performed with an accuracy rate of 75.0% (24/32) on the Shape trials and with 100% accuracy on the 32 Location trials, both of which were significantly ($p < 0.05$) above chance levels of 50% (see alsoThaler et al., 2011). This Shape-trial performance was similar to EB's other chamber-recorded Shape-trial performance in Experiment 1. While LB showed a trend to be above chance levels

in terms of his Shape task accuracy [65.6% (21/32), $p = 0.077$, two-tailed *t*-test], his Location performance was at chance levels of 50% (16/32).

4.2.2. Shape-Location (SL) Experiment

S > Baseline (Silence) ∩ L > Baseline (Silence). Common areas of Shape and Location echo processing compared to silence in EB included bilateral primary auditory cortex, insula, superior parietal lobule, middle occipital gyrus, lingual gyrus, Supplementary Motor area and cerebellum (See Figure 5, Table S8a). This auditory/echo activation was especially strong in EB's right hemisphere, as we previously reported (Thaler et al., 2011), with extensive activation throughout the right occipital lobe (cuneus and middle occipital gyrus) that extended anteriorly into the right auditory cortex and dorsally towards the inferior parietal lobe. EB's left thalamus also showed strong activation for this sound versus silence contrast. Though not as extensive or right-biased, LB also showed a wide network of brain areas activated by this same contrast. These included bilateral auditory cortex, insula, middle temporal and middle occipital gyri, cuneus, precuneus and inferior and superior parietal lobes, Supplementary Motor area, and frontal gyrus (see Figure S4 and Table S9a).

S > L ∩ S > Baseline (Silence). For EB, brain regions that showed significantly greater BOLD activity for the S condition relative to the L task as well as the silent baseline condition included the rostral portions of the left and right cuneus, a region of the anterior right insula and IFG, as well as the right fusiform gyrus and the right middle frontal gyrus and left precentral gyrus (Figure 5, Table S8b). On the other hand, LB did not show any shape-specific activation in ventral occipital regions (see Supplemental Figure S4, Table

S9b). Rather, Shape-specific activity was located in the left precuneus and angular gyrus, and, like EB, in the middle frontal and precentral gyri.

L > S ∩ L > Baseline (Silence). For EB, no brain region demonstrated significantly greater Location-specific activity. The largest near-significant area of activation (38 voxels at the $p < 0.01$ level, or 218 voxels at the $p < 0.05$ level) was located in the right parietal lobe (Brodmann Area 7 of the precuneus; see Figure 5 and Table S8c). LB, on the other hand, showed a great deal of location-specific activity (see Figure S4 and Table S9c), located in the IPL (predominately right hemisphere), right cuneus, bilateral middle temporal gyrus, right supramarginal gyrus, left lingual gyrus, bilateral middle frontal and precentral gyri, and in the cingulate gyrus.

Insert Figure 5 about here

5. Discussion

Even though EB was listening to the same set of echolocation recordings, attending to the shape as compared to the material (Experiment 1) or location (Experiment 2) features derived from the echoes of the otherwise silent objects in those recordings elicited greater BOLD activation in his occipital cortex. This activation was located not only in anterior and lateral regions typically associated with shape processing, but also in regions commonly referred to as primary visual cortex in sighted individuals. What is more, Experiment 1 showed that for many of these occipital regions, the Baseline task of passively listening to the same echolocation recordings with the click echoes removed, resulted in a level of BOLD activity that was mid-way between the two active echo tasks

(Shape and Material), arguing against a mere effect of task difficulty. Our results therefore suggest that the echo-related occipital lobe activation previously observed for EB (Thaler et al., 2011) does not appear to reflect a general pattern of echo-processing. Rather, the echo-processing, at least outside of primary 'visual' cortex, appears to engage feature-specific brain areas that are typically found to be active in the processing of visual and source-based auditory features. Finally, the fact that neither the congenital (Exp 1) nor the late-blind (Exp 2) echolocating experts showed the same type of activation that EB did in early occipital areas suggests that extensive echolocation training, from a young and perhaps even critical stage of neurological development, plays a strong role in establishing how echo-processing is instantiated in the brain (e.g., topographic mapping of objects in the environment as conveyed through echo information).

5.1 Shape-specific Processing

In Experiment 1, EB's Shape > Material activation in bilateral fusiform gyrus and right MOG, proximal to his Shape > Location area in Experiment 2 (see Figure 5), is consistent with the role of ventrolateral occipital brain regions in processing object form (Cant et al., 2009; Grill-Spector et al., 2001; Haxby et al., 2001; Malach et al., 1995). That said, the activation in Experiment 1 was not as strong as what one may have expected (e.g., this area did not show up in the Shape conjunction contrast) and echolocator CB did not show shape-specific activity in these lateral regions either. Task performance may have influenced these results. While neither EB nor CB performed at above chance levels on the Shape task, EB but not CB, showed improvement on chamber-recorded sounds and this corresponded to increased activity in these

fusiform/MOG regions. In addition, the common areas of BOLD activation during the Shape and Material tasks that occurred in EB's left LOC (and in the right posterior MTG of CB) relative to the Place task, suggests that the Shape and Material tasks were not entirely independent of one another. In fact, EB had noted that the task of separating an object's shape from its surface properties was a somewhat unnatural use of echolocation for him in the sense that in the real world, a similar task would be accomplished by reaching out and touching the object. This point also underscores the relative dissociation between echo-derived shape information (useful for extrapersonal space) from that of haptics (useful for peripersonal space), of which associations with the latter often play a strong role in driving LOC activation (Amedi et al., 2001). Moreover, for smaller objects such as those used in the current experiment, shape and surface composition features likely begin to affect the echo characteristics in similar ways. For example, just as the concavity of the bowl will serve to amplify the returning echo relative to that of a flat surface, so too will the aluminum foil relative to the cloth towel. Accordingly, it is likely that success on either the Shape or Material task was somewhat dependent on an awareness or consideration of both features, as well as prior knowledge of the conditions that had been used.

With respect to the Shape task in Experiment 2, EB also showed shape-specific activity in the right fusiform gyrus, extending into the MOG where shape-specific activity was found in Experiment 1 (see Figure 4). Though this activation was slightly medial to the shape-specific area in Experiment 1, the conjunction analysis of shape and location processing clearly activated the same region of the right MOG. Similarly, while LB in Experiment 2 did not show echo shape-specific activation in his ventro-lateral

occipital regions, the conjunction analysis of shape and location also showed bilateral MOG/LOC activity. As was the case with Experiment 1, it may be that echo-derived judgments of location rely on at least a preliminary analysis of object shape features.

In addition to LOC, other areas of common echo activity within the Shape and Material tasks in Experiment 1 included the angular gyrus (EB and CB) and posterior hippocampus (EB only). Activation of the angular gyrus has been associated with semantic language retrieval (Binder, Westbury, McKiernan, Possing, & Medler, 2005; Price, 2010), mental arithmetic related to mapping problems onto solutions in stored memory (Grabner, Ansari, Koschutnig, Reishofer, & Ebner, 2011), as well as in the detection of visuoauditory environmental sound incongruencies (Noppeney, Josephs, Hocking, Price, & Friston, 2008), so the angular gyrus may act as a 'way-station' between traditional auditory processing areas, and co-opted 'visual' cortical regions used to analyze echo information. The posterior hippocampus activation can also be understood in a similar manner, given its prominent role in memory and spatial navigation (Maguire et al., 2000; Poppenk & Moscovitch, 2011).

Relative to the Shape task, the Material task of the current study generated significantly greater activity in EB's right supramarginal gyrus, possibly indicating a 'material-specific' role for these regions in his echo processing. However, these observations must be qualified by the fact that those areas were not significantly activated when subjected to a more stringent conjunction contrast involving the 'echoless' control sounds, nor were they activated preferentially by CB's echo-Material processing. Moreover, the Material task did not elicit any greater amount of BOLD response than did the Baseline or the Place task. In fact, supramarginal gyrus activation during the Material

task was less than that of the Place task. This pattern of activity was the same as that of the accuracy performance among the different tasks. In other words, the similarity of BOLD activity with that of EB's behavioural performance (poorest performance on Shape, then Material, then Place task) suggests that the supramarginal gyrus activity may relate more closely to EB's behavioural performance across the various types of tasks rather than material-specific echo processing per se. In keeping with this, supramarginal gyrus activation is often associated with spatial mapping processes, being involved in remapping visual spatial information across saccades (Russell et al., 2010), as well as in circumstances in which attentional capture by memory content is maximal (e.g., strong vs. weak memories, vividly recollected versus familiar memories, etc., \Ciaramelli, 2008 #6334}.

Finally, with respect to Experiment 2's Shape-Location echo processing, it is interesting to note that the only cortical region in EB where echo processing tended to be greater for the Location task relative to the Shape task, was in the right precuneus (Figure 5). LB also showed activation in a very proximal region in his right precuneus and IPL (Figure S4). Thus, as with real sound source localization (Arnott & Alain, 2011; Arnott et al., 2004), echo-based object localization seems to invoke similar regions of the parietal cortex.

5.2 Topographic representations?

While activation in fusiform and LOC regions of the occipital lobe in response to shape and material echo processing can be explained in terms of cortical functional specialization as outlined above, the strong activation of the occipital pole (bilateral

BA17) in the Shape relative to the Material task for EB (absent for CB) is not as obvious (see Figure 3). Our working hypothesis that will require more formal experimentation is that EB's BA17 activation in response to echolocation shape-extraction reflects topographic organization of echo-derived objects as well as the spatial layout of the environment. In sighted individuals, a functional hallmark of primary visual cortex is its retinotopic organization whereby increasing visual field eccentricities are represented at progressively more rostral regions from the occipital pole, and where, owing to the cross-over projections from the retinae to visual cortex, left and right visual fields are predominately represented in contralateral occipital hemispheres (Daniel & Whitteridge, 1961; Sereno et al., 1995; Tootell, Silverman, Switkes, & De Valois, 1982).

With respect to eccentricity, Experiment 1 demonstrated that caudal occipital areas in EB's occipital pole showed increased BOLD activity when he extracted the shape as opposed to the material composition of the object located directly in front of him (see Figure 3). On the other hand, when EB completed a different shape experiment in which the objects were placed 20° to the left or right of straight ahead (Experiment 2), shape-specific activation in occipital cortex was located more rostrally along the calcarine sulcus (see Figure 5), and was not present in LB (see Figure S4). A more direct comparison of EB's experimental results is illustrated in the top panel of Figure 6 where results from Experiments 1 and 2 are overlaid on the same brain image. Furthermore, in Experiment 1 when the task involved processing the overall spatial/environmental layout (i.e., the Place task), BOLD activity was observed along the extent of the calcarine sulcus. However, when this Place task activity was contrasted with the other tasks of Experiment 1 that required processing of the object directly in front of EB, the BOLD

increase no longer occurred in the occipital pole, but was focused in regions usually implicated in the processing of the 'visual periphery'; i.e., the rostral aspect of the calcarine cortex (see Figure 2 inset). Similarly, in our previous study, we found activation along the extent of the calcarine cortex when EB identified very large objects from a distance of approximately 1 m directly in front of him (i.e., a car, a tree, and a lamppost, Thaler et al., 2011). From a topographic eccentricity perspective, objects that subtend a larger visual angle should be expected to stimulate a greater range of topographic cortex. Thus, that finding too is consistent with the idea that there may exist some sort of eccentricity mapping in EB's early visual cortex during certain types of echolocation processing.

Insert Figure 6 about here

With respect to contralateral representation of the hemifield, we have previously reported (Thaler et al., 2011) that EB's calcarine activity during Experiment 2 was significantly stronger in the hemisphere contralateral to the location of the silent objects that he was identifying (see Figure 6 bottom). This result is consistent with the notion that there exists some sort of phase-reversed angular mapping in EB's occipital cortex during certain types of echolocation processing. In summary, there is converging evidence for the idea that echolocation-related activity in EB's calcarine cortex may be organized in a manner similar to the way light related activity is organized in sighted people's calcarine cortex, i.e. by eccentricity and angle.

5.3 Other echolocators

Whether these BOLD activation patterns would be found in other expert blind (especially early blind) echolocators apart from EB deserves further study. In Experiment 1, the congenitally blind echolocator (i.e., CB) did not show activation of the occipital pole in response to echo processing, although he did show some weak shape-specific echo activation in more rostral medial regions. Furthermore, the late blind echolocation expert participating in Experiment 2 (i.e., LB) showed neither the shape-specific activation of the occipital pole, nor the topographic response to lateralized sounds that EB did (see also, Thaler et al., 2011).

Thus, while the feature-specific processing patterns found in EB may occur in other blind echolocators, the topographic-like activation of early 'visual' cortex may very well be specific to EB and other echolocating individuals who lost their sight very early in life *and* began using echolocation soon after. Indeed, a growing body of evidence suggests that early visual experience can fundamentally change how non-visual sensory input is processed in occipital areas (Noppeney, 2007; Röder, Kusmierek, Spence, & Schicke, 2007). As Collignon and colleagues (2011) point out, it is known that the number of synapses within human visual cortex increases from birth to a point where maximum density is achieved at 8 months of age. Thereafter, a decade-long process of synaptic pruning begins in which nearly half (i.e., 40%) of these synapses are removed (Huttenlocher & de Courten, 1987). The surgical removal of EB's eyes at age 7 and 13-months, followed by his commencement of active echolocation shortly thereafter, may therefore have occurred at a critical point in his life when his occipital cortex and its retinotopic scaffolding had been established/honed by a year of visual input, yet was still

highly malleable for integration with other sensory input. Indirect support for this is also derived from observations of retinotopic reorganization of occipital cortex for tactile patterns in a visually impaired adult whose visual acuity was compromised at the relatively early age of 6 years due to corneal opacification (Cheung, Fang, He, & Legge, 2009).

Related to this, another important question for future study is whether EB's brain represents localizable auditory stimuli (i.e., sound sources) in a similar topographic manner in primary 'visual' cortex? Such data would speak to the question of whether EB's echolocation processing is markedly different from how he processes other auditory spatial input. This might also provide some perspective on whether early auditory (i.e., echolocation) intervention in young blind individuals can fundamentally change the functional organization or functional use of early 'visual' areas.

Returning to the idea of latent, multisensory features of the brain (c.f., Pascual-Leone & Hamilton, 2001) and whether echolocation in the blind takes advantage of these features, it will also be of interest to test congenitally blind individuals who echolocate, in order to determine whether the echo activations that we have observed in early and late blind individuals are dependent on some form of visual experience. There are numerous accounts of congenitally blind individuals who show functional specialization in the occipital lobe, and it has recently been argued that some regions of the occipital lobe, most notably the right cuneus, do not require visual experience in order to develop specialization for the processing of spatial information and to be functionally integrated in a pre-existing brain network dedicated to such an ability (Collignon, Champoux et al., 2011). The right dorsal occipital lobe in particular is known to be prominently active

when blind but not sighted individuals localize sounds (Collignon, Lassonde, Lepore, Bastien, & Veraart, 2007; Collignon, Vandewalle et al., 2011; Renier et al., 2010; Weeks et al., 2000), and it is interesting to note that both EB and LB showed strong activation of this region when lateralized objects were being discerned through echoes (Figures 5 and S4), but that this area was not activated by either EB or CB when there was no variation in object location (i.e., the Shape and Material task of Experiment 1).

5.4 Auditory cortex and echolocation in different acoustic environments:

But what about echo-specific activity in auditory cortex? On the one hand the lack of differential activity in auditory cortex is surprising given that echolocation relies on the analysis of fine-grained acoustic features (i.e., the characteristics of the click echoes); a function that the auditory cortices are exquisitely capable of (Nourski & Brugge, 2011). At the same time, the acoustic energy in the contrast conditions was always carefully controlled, either being exactly the same as in the contrasts in which the listener extracted different features from the same echolocation recording (e.g., Shape versus Material, Shape versus Location), or very nearly the same as in the contrasts of echolocation recordings with the recordings where only the click echoes were removed.

One possibility is that our fMRI design was limited in its ability to register subtle BOLD differences in auditory cortex. Specifically, even though we used a sparse sampling design to avoid that scanner noise would mask the auditory stimulus, in particular the echo component, we only used a two second interstimulus interval between scanner noise offset and the experimental stimuli of the next trial. Thus, our paradigm did not provide the 9-12 s delay of silence that is required for the BOLD signal in primary

and secondary auditory cortices to return to baseline levels (Hall et al., 2000). For this reason it is possible that our design may not have been optimal for detecting subtle signal changes in the auditory cortex. The fact that the echo (i.e., Shape and Material tasks) versus Baseline task did not reveal any activity in Heschl's gyrus despite the fact that the baseline condition contained less acoustic energy (i.e., no click echoes) supports this argument. Nevertheless, the experimental design was clearly sensitive enough to register large BOLD activity differences elsewhere (i.e., occipital cortex), suggesting that, at least in the blind echolocators that we have tested, large and reliable activity differences related to the interpretation of echo information can be found elsewhere in the brain. Given that sighted individuals can be trained to echolocate (Teng & Whitney, 2011), it will be of interest to examine the echo-related brain activity in such individuals to determine whether the neural activity patterns are similar to those found in blind participants, or if they rely more on auditory cortices.

Outside of the laboratory, different auditory environments pose different challenges for echolocation and presumably auditory cortex. For example, noisier and/or more reverberant environments are more likely to mask the clicks and especially their echoes. The acoustic differences between the chamber and alcove locations therefore provided a unique opportunity for examining the effect of signal quality on echo processing. An RMS power analysis confirmed the perception that EB's tongue click recordings in the chamber were audibly more distinct from the background noise than they were for the alcove recordings (not true for CB, perhaps due to differences in click amplitude and/or microphone depth and orientation during different recording sessions). Even though the chamber stimuli contained an overall smaller average RMS level (reflected as greater

alcove versus chamber baseline activity during the Baseline task for both EB and CB), EB's chamber stimuli contained greater maximum and minimum RMS power levels than alcove stimuli, indicating a better signal to noise ratio. EB's performance on these recordings was consistent with this as he performed significantly better on both the Shape and Material trials when the stimuli had been recorded in the chamber as opposed to the alcove (n.b., he performed perfectly on all Place trials). Accordingly, one can ask how EB's echo-related brain activity differs when the clicks and their echoes are more audible from the background noise.

In this regard, the BOLD contrast of EB's chamber versus alcove stimuli revealed some interesting results. When comparing these recording types during echo processing (i.e., collapsing across Shape and Material conditions), significant activity in bilateral Heschl's gyrus as well as the occipital lobe (i.e., cuneus, MOG, fusiform gyrus) was observed, with the BOLD activity being larger for the chamber compared to the alcove recordings. Given that the alcove recordings had an overall greater mean amplitude, these results indicate that the Heschl's gyrus activation was not related to overall acoustic energy (Hall et al., 2001; Jäncke, Shah, Posse, Grosse-Ryuken, & Müller-Gärtner, 1998). Moreover, the fact that neither the Place nor the Baseline task showed a chamber greater than alcove activation in these same areas, indicates that the activity was specific to echo processing. CB also showed a similar pattern of activity. These results suggest that an important role of auditory cortex in echo processing is in representing and/or extracting the echo information from the background noise. This interpretation is supported by fMRI findings showing that Heschl's gyrus activity increases with increasing signal

audibility, even when the overall loudness level is held constant (Ernst, Verhey, & Uppenkamp, 2008).

6. Summary:

In conclusion, we have shown that the extraction of a silent object's shape by a blind human echolocation expert selectively recruits regions of occipital cortex, including areas traditionally involved in visual shape processing. Moreover, the pattern of activation in his occipital cortex is such that it supports the idea of an echolocation-derived topographic representation of that object in the environment. Finally, this activation appears to be dependent on the ability of the auditory cortex to reliably extract the echo information from the background noise.

Acknowledgments

The authors wish to thank Adam Shaible, Juan Ruiz and Brian Bushway of World Access for the Blind for helpful comments on experimental design, and Dr. Haitao Yang for technical assistance. This work was supported by a grant from the Canadian Institutes of Health Research (MAG).

References

Amedi, A., Jacobson, G., Hendler, T., Malach, R., & Zohary, E. (2002). Convergence of visual and tactile shape processing in the human lateral occipital complex. *Cereberal Cortex, 12*(11), 1202-1212.

Amedi, A., Malach, R., Hendler, T., Peled, S., & Zohary, E. (2001). Visuo-haptic object-related activation in the ventral visual pathway. *Nature Neuroscience, 4*(3), 324-330.

Amedi, A., Stern, W. M., Camprodon, J. A., Bermpohl, F., Merabet, L., Rotman, S. (2007). Shape conveyed by visual-to-auditory sensory substitution activates the lateral occipital complex. *Nature Neuroscience, 10*(6), 687-689.

Arnott, S. R., & Alain, C. (2011). The auditory dorsal pathway: orienting vision. *Neuroscience and Biobehavioral Reviews, 35*(10), 2162-2173.

Arnott, S. R., Binns, M. A., Grady, C. L., & Alain, C. (2004). Assessing the auditory dual-pathway model in humans. *NeuroImage, 22*(1), 401-408.

Arnott, S. R., Cant, J. S., Dutton, G. N., & Goodale, M. A. (2008). Crinkling and crumpling: an auditory fMRI study of material properties. *NeuroImage, 43*(2), 368-378.

Binder, J. R., Westbury, C. F., McKiernan, K. A., Possing, E. T., & Medler, D. A. (2005). Distinct brain systems for processing concrete and abstract concepts. *Journal of Cognitive Neuroscience, 17*(6), 905-917.

Burton, H., Snyder, A. Z., Diamond, J. B., & Raichle, M. E. (2002). Adaptive changes in early and late blind: a FMRI study of verb generation to heard nouns. *Journal of Neurophysiology, 88*(6), 3359-3371.

Cant, J. S., Arnott, S. R., & Goodale, M. A. (2009). fMR-adaptation reveals separate processing regions for the perception of form and texture in the human ventral stream. *Experimental Brain Research, 192*(3), 391-405.

Cant, J. S., & Goodale, M. A. (2011). Scratching beneath the surface: new insights into the functional properties of the lateral occipital area and parahippocampal place area. *The Journal of Neuroscience, 31*(22), 8248-8258.

Cavina-Pratesi, C., Kentridge, R. W., Heywood, C. A., & Milner, A. D. (2010). Separate processing of texture and form in the ventral stream: evidence from FMRI and visual agnosia. *Cereberal Cortex, 20*(2), 433-446.

Cheung, S. H., Fang, F., He, S., & Legge, G. E. (2009). Retinotopically specific reorganization of visual cortex for tactile pattern recognition. *Current Biology, 19*(7), 596-601.

Collignon, O., Champoux, F., Voss, P., & Lepore, F. (2011). Sensory rehabilitation in the plastic brain. *Progress in Brain Research, 191*, 211-231.

Collignon, O., Lassonde, M., Lepore, F., Bastien, D., & Veraart, C. (2007). Functional cerebral reorganization for auditory spatial processing and auditory substitution of vision in early blind subjects. *Cerebral Cortex, 17*(2), 457-465.

Collignon, O., Vandewalle, G., Voss, P., Albouy, G., Charbonneau, G., Lassonde, M. (2011). Functional specialization for auditory-spatial processing in the occipital cortex of congenitally blind humans. *Proceedings of the National Academy of Sciences of the United States of America, 108*(11), 4435-4440.

Collignon, O., Voss, P., Lassonde, M., & Lepore, F. (2009). Cross-modal plasticity for the spatial processing of sounds in visually deprived subjects. *Experimental Brain Research, 192*(3), 343-358.

Cox, R. W. (1996). AFNI: software for analysis and visualization of functional magnetic resonance neuroimages. *Computers and Biomedical Research, 29*(3), 162-173.

Daniel, P. M., & Whitteridge, D. (1961). The representation of the visual field on the cerebral cortex in monkeys. *The Journal of Physiology, 159*, 203-221.

Ernst, S. M., Verhey, J. L., & Uppenkamp, S. (2008). Spatial dissociation of changes of level and signal-to-noise ratio in auditory cortex for tones in noise. *NeuroImage, 43*(2), 321-328.

Grabner, R. H., Ansari, D., Koschutnig, K., Reishofer, G., & Ebner, F. (2011). The function of the left angular gyrus in mental arithmetic: Evidence from the associative confusion effect. *Human Brain Mapping, [Epub ahead of print], http://www.ncbi.nlm.nih.gov/entrez/query.fcgi?cmd=Retrieve&db=PubMed&dopt=Citation&list_uids=22125269*.

Grill-Spector, K., Kourtzi, Z., & Kanwisher, N. (2001). The lateral occipital complex and its role in object recognition. *Vision Research, 41*(10-11), 1409-1422.

Hall, D. A., Haggard, M. P., Akeroyd, M. A., Palmer, A. R., Summerfield, A. Q., Elliott, M. R. (1999). "Sparse" temporal sampling in auditory fMRI. *Human Brain Mapping, 7*(3), 213-223.

Hall, D. A., Haggard, M. P., Akeroyd, M. A., Summerfield, A. Q., Palmer, A. R., Elliott, M. R. (2000). Modulation and task effects in auditory processing measured using fMRI. *Human Brain Mapping, 10*(3), 107-119.

Hall, D. A., Haggard, M. P., Summerfield, A. Q., Akeroyd, M. A., Palmer, A. R., & Bowtell, R. W. (2001). Functional magnetic resonance imaging measurements of sound-level encoding in the absence of background scanner noise. *The Journal of the Acoustical Society of America, 109*(4), 1559-1570.

Haxby, J. V., Gobbini, M. I., Furey, M. L., Ishai, A., Schouten, J. L., & Pietrini, P. (2001). Distributed and overlapping representations of faces and objects in ventral temporal cortex. *Science, 293*(5539), 2425-2430.

Huttenlocher, P. R., & de Courten, C. (1987). The development of synapses in striate cortex of man. *Human Neurobiology, 6*(1), 1-9.

James, T. W., Humphrey, G. K., Gati, J. S., Servos, P., Menon, R. S., & Goodale, M. A. (2002). Haptic study of three-dimensional objects activates extrastriate visual areas. *Neuropsychologia, 40*(10), 1706-1714.

James, T. W., Stevenson, R. A., Kim, S., Vanderklok, R. M., & James, K. H. (2011). Shape from sound: evidence for a shape operator in the lateral occipital cortex. *Neuropsychologia, 49*(7), 1807-1815.

Jäncke, L., Shah, N. J., Posse, S., Grosse-Ryuken, M., & Müller-Gärtner, H. W. (1998). Intensity coding of auditory stimuli: an fMRI study. *Neuropsychologia, 36*(9), 875-883.

Kim, J. K., & Zatorre, R. J. (2011). Tactile-auditory shape learning engages the lateral occipital complex. *The Journal of Neuroscience, 31*(21), 7848-7856.

Lewis, J. W., Brefczynski, J. A., Phinney, R. E., Janik, J. J., & DeYoe, E. A. (2005). Distinct cortical pathways for processing tool versus animal sounds. *Journal of Neuroscience, 25*(21), 5148-5158.

Maguire, E. A., Gadian, D. G., Johnsrude, I. S., Good, C. D., Ashburner, J., Frackowiak, R. S. (2000). Navigation-related structural change in the hippocampi of taxi drivers. *Proceedings of the National Academy of Sciences of the United States of America, 97*(8), 4398-4403.

Malach, R., Reppas, J. B., Benson, R. R., Kwong, K. K., Jiang, H., Kennedy, W. A. (1995). Object-related activity revealed by functional magnetic resonance imaging in human occipital cortex. *Proceedings of the National Academy of Sciences of the United States of America, 92*(18), 8135-8139.

Noppeney, U. (2007). The effects of visual deprivation on functional and structural organization of the human brain. *Neuroscience and Biobehavioral Reviews, 31*(8), 1169-1180.

Noppeney, U., Josephs, O., Hocking, J., Price, C. J., & Friston, K. J. (2008). The effect of prior visual information on recognition of speech and sounds. *Cerebral Cortex, 18*(3), 598-609.

Nourski, K. V., & Brugge, J. F. (2011). Representation of temporal sound features in the human auditory cortex. *Reviews in the Neurosciences, 22*(2), 187-203.

Pascual-Leone, A., & Hamilton, R. (2001). The metamodal organization of the brain. *Progress in Brain Research, 134*, 427-445.

Poppenk, J., & Moscovitch, M. (2011). A hippocampal marker of recollection memory ability among healthy young adults: Contributions of posterior and anterior segments. *Neuron, 72*(6), 931-937.

Price, C. J. (2010). The anatomy of language: a review of 100 fMRI studies published in 2009. *Annals of the New York Academy of Sciences, 1191*, 62-88.

Ptito, M., Matteau, I., Zhi Wang, A., Paulson, O. B., Siebner, H. R., & Kupers, R. (2012). Crossmodal recruitment of the ventral visual stream in congenital blindness. *Neural Plasticity, 2012*, 304045.

Renier, L. A., Anurova, I., De Volder, A. G., Carlson, S., VanMeter, J., & Rauschecker, J. P. (2010). Preserved functional specialization for spatial processing in the middle occipital gyrus of the early blind. *Neuron, 68*(1), 138-148.

Röder, B., Kusmierek, A., Spence, C., & Schicke, T. (2007). Developmental vision determines the reference frame for the multisensory control of action. *Proceedings of the National Academy of Sciences, 104*(11), 4753-4758.

Rojas, J. A. M., Hermosilla, J. A., Montero, R. S., & Espi, P. L. L. (2009). Physical analysis of several organic signals for human echolocation: Oral vacuum pulses. *Acta Acustica United with Acustica, 95*(2), 325-330. doi: 10.3813/aaa.918155

Russell, C., Deidda, C., Malhotra, P., Crinion, J. T., Merola, S., & Husain, M. (2010). A deficit of spatial remapping in constructional apraxia after right-hemisphere stroke. *Brain, 133*(Pt 4), 1239-1251.

Schenkman, B. N., & Nilsson, M. E. (2010). Human echolocation: Blind and sighted persons' ability to detect sounds recorded in the presence of a reflecting object. *Perception, 39*(4), 483-501.

Sereno, M. I., Dale, A. M., Reppas, J. B., Kwong, K. K., Belliveau, J. W., Brady, T. J. (1995). Borders of multiple visual areas in humans revealed by functional magnetic resonance imaging. *Science, 268*(5212), 889-893.

Stoffregen, T. A., & Pittenger, J. B. (1995). Human echolocation as a basic form of perception and action. *Ecological Psychology, 7*(3), 181-216.

Talairach, J., & Tournoux, P. (1988). *Co-planar stereotaxic atlas of the human brain*. New York: Thieme Medical Publishers.

Teng, S., Puri, A., & Whitney, D. (2012). Ultrafine spatial acuity of blind expert human echolocators. *Experimental Brain Research, 216*(4), 483-488.

Teng, S., & Whitney, D. (2011). The acuity of echolocation: Spatial resolution in the sighted compared to expert performance. *Journal of Visual Impairment and Blindness, 105*(1), 20-32.

Thaler, L., Arnott, S. R., & Goodale, M. A. (2011). Neural correlates of natural human echolocation in early and late blind echolocation experts. *PLoS One, 6*(5), e20162.

Tootell, R. B., Silverman, M. S., Switkes, E., & De Valois, R. L. (1982). Deoxyglucose analysis of retinotopic organization in primate striate cortex. *Science, 218*(4575), 902-904.

Ungerleider, L. G., Courtney, S. M., & Haxby, J. V. (1998). A neural system for human visual working memory. *Proceedings of the National Academy of Sciences of the United States of America, 95*(3), 883-890.

Weeks, R., Horwitz, B., Aziz-Sultan, A., Tian, B., Wessinger, C. M., Cohen, L. G. (2000). A positron emission tomographic study of auditory localization in the congenitally blind. *Journal of Neuroscience, 20*(7), 2664-2672.

Figure Captions

Figure 1. Experimental design for Experiments 1 (top) and 2 (bottom). Enlarged view of trial structure is shown in the middle, and is also applicable to Experiment 2. Time is denoted from left to right in seconds (s). Dotted curve represents schematic of the brain's blood-oxygenated level dependent (BOLD) response to the click stimuli relative to the onset of the functional magnetic resonance imaging scan. "resp. cue" = response cue.

Figure 2. Haemodynamic activity associated with general echo processing relative to control tasks for EB in Experiment 1 (i.e., Shape and Material versus Place and Baseline). For selected activation regions, mean beta weight values are plotted for each task: Shape (red), Material (blue) and Place (green). Error bars represent standard error of the mean. L/R Ang. Gy. = left/right Angular Gyrus; L Pos. Hipp. = left posterior Hippocampus; LOC = Lateral Occipital Complex; Parahipp. = Parahippocampus; R Calc. = right Calcarine Sulcus. Dashed line inset (bottom right) contains Place task-specific activity (i.e., Place > Baseline ∩ Place > Shape ∩ Place > Material) in the right calcarine sulcus. Minimum cluster size set at 250 voxels. Talairach slice orientation (X, Y, or Z) in mm.

Figure 3. Task dependent haemodynamic activity associated with EB's Shape versus Material echo tasks of Experiment 1. Results of conjunction contrast Shape > Material ∩ Shape > Baseline are overlaid (yellow). Overlap of the two contrasts is shown in orange. Minimum cluster size set at 250 voxels. Talairach slice orientation (X, Y, or Z) in mm. Bottom: plots of average beta weight signal values extracted from subsections of activated Shape versus Material clusters including: L Fusiform Gyr., L IOG, R IOG, R MOG, L Lingual Gyr. , R Lingual Gyr., Angular Gyr. Mean signal values are plotted separately for chamber Shape trials (chS), alcove Shape trials (alS), chamber Material

trials (chM), alcove Material trials (alM), chamber Place trials (chP), and alcove Place trials (alP). Error bars represent standard error of the mean. Abbreviations: L = left; R = right; Gyr. = gyrus; IOG = Inferior Occipital Gyrus; MOG = Middle Occipital Gyrus; Supramarg. = Supramarginal.

Figure 4. a) Echo-related haemodynamic activity (i.e., Shape and Material tasks) according to the environment that the echolocation stimulus was recorded in (i.e., anechoic chamber or hallway alcove). Contrast of chS + chM vs. alS + alM. Axial (Z = 9 mm) and coronal (Y = 19 mm) slices are shown. Average beta weight signal values extracted from subsections of the left and right auditory cortex are plotted separately for chamber Shape (chS), alcove Shape (alS), chamber Material (chM), alcove Material (alM), chamber Place (chP), and alcove Place (alP) trials. Error bars represent standard error of the mean. b) Haemodynamic activity that was greater for the chamber relative to the alcove recordings. Results are overlaid separately for the Shape (red), Material (blue) and Place (green) tasks. Nb: no significant Place activity is present. Left (L) and Right (R) Heschl's Gyrus are indicated (violet). Minimum cluster size set at 250 voxels.

Figure 5. Task dependent haemodynamic activity associated with EB's Shape (S) and Location (L) echo tasks of Experiment 2 when the echolocation object was located 20° to the left or right of straight-ahead. Common areas of activity between S and L echo processing relative to the silent baseline are shown in pink. S-specific echo activity is shown in orange, and L-specific echo activity is shown in blue. For comparison, the S-specific activation in the right Fusiform/LOC from EB in Experiment 1 is overlaid in brown. Minimum cluster size set at 250 voxels, with the exception of the 218 voxel L-

specific cluster in the right Precuneus. Talairach slice orientation in mm. LOC = Lateral Occipital Complex; Gyr. = Gyrus.

Figure 6. Shape-specific echo results from Figures 2 and 4 re-plotted on Talairach sagittal slices of the left (L) and right (R) occipital lobe. Yellow represents activity related to object directly in front of EB (Experiment 1). Red represents activity associated with a lateralized object (Experiment 2). Bottom: Plot of BOLD activity (mean Beta values) in the left and right calcarine ROIs according to the side of space that the object was located during Experiment 2 (adapted from Thaler et al., 2011). ** = $p <$ 0.001.

Figure 1

Click here to download high resolution image

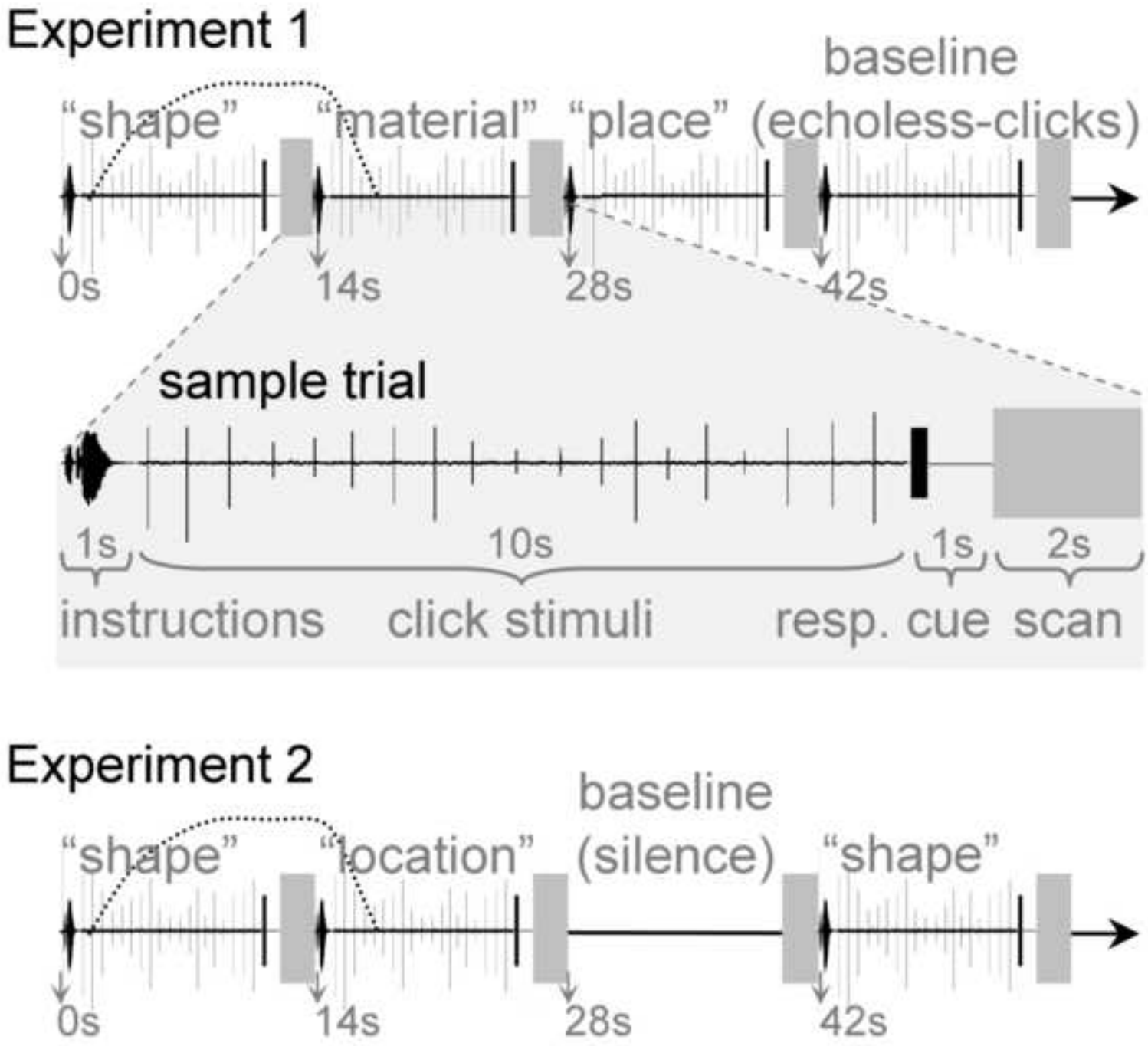

Figure 2

Click here to download high resolution image

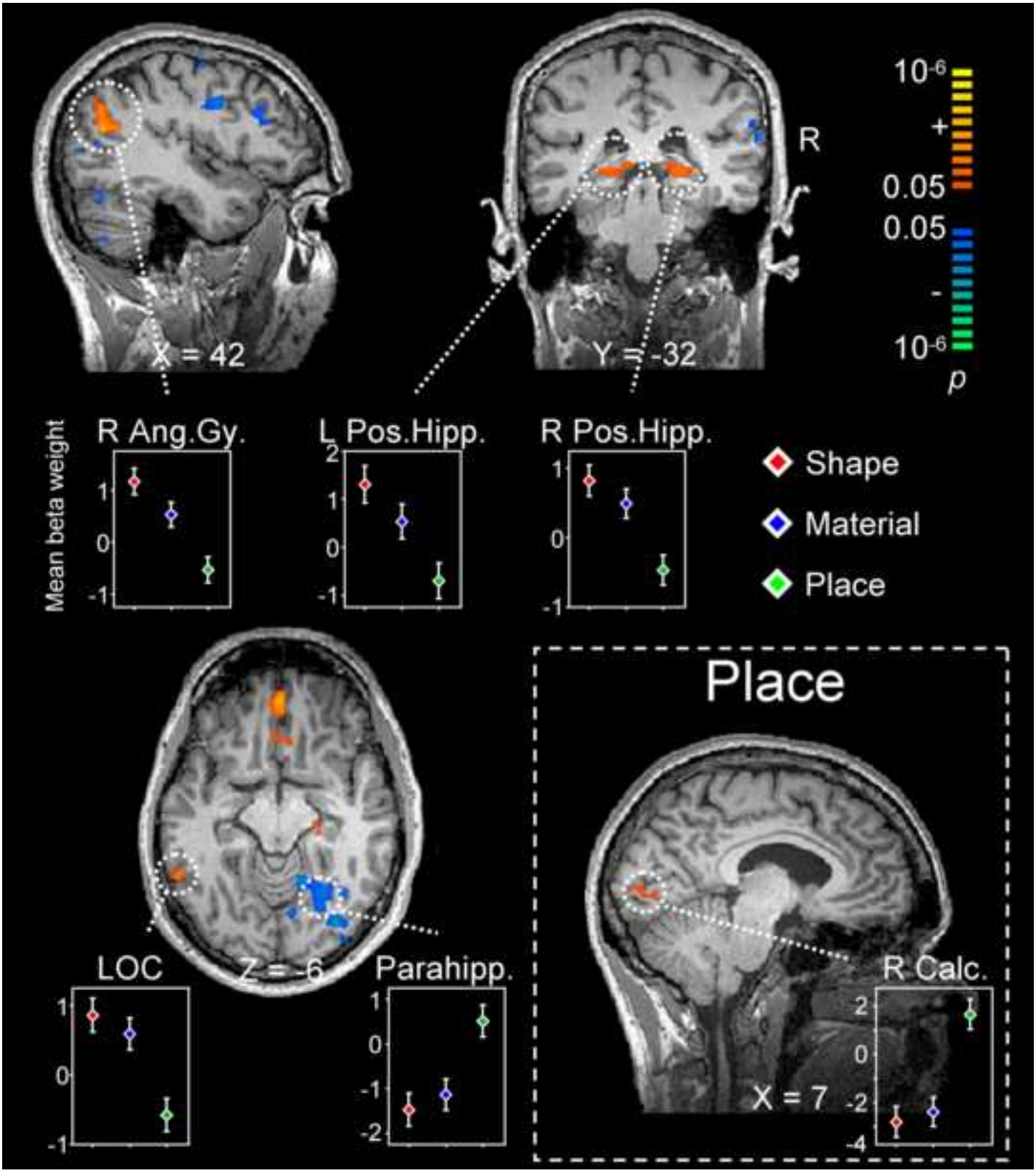

Figure 3

Click here to download high resolution image

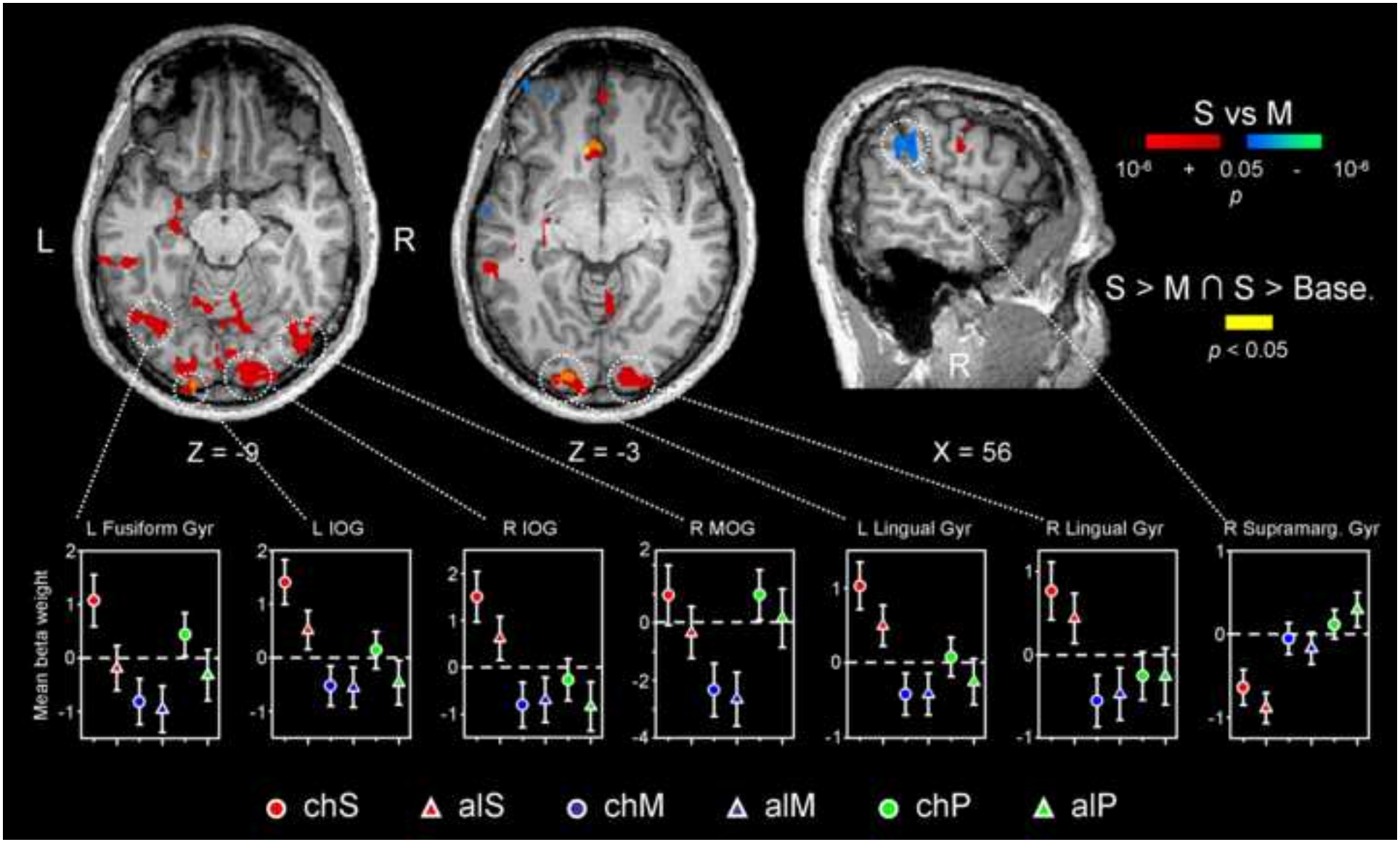

Figure 4

Click here to download high resolution image

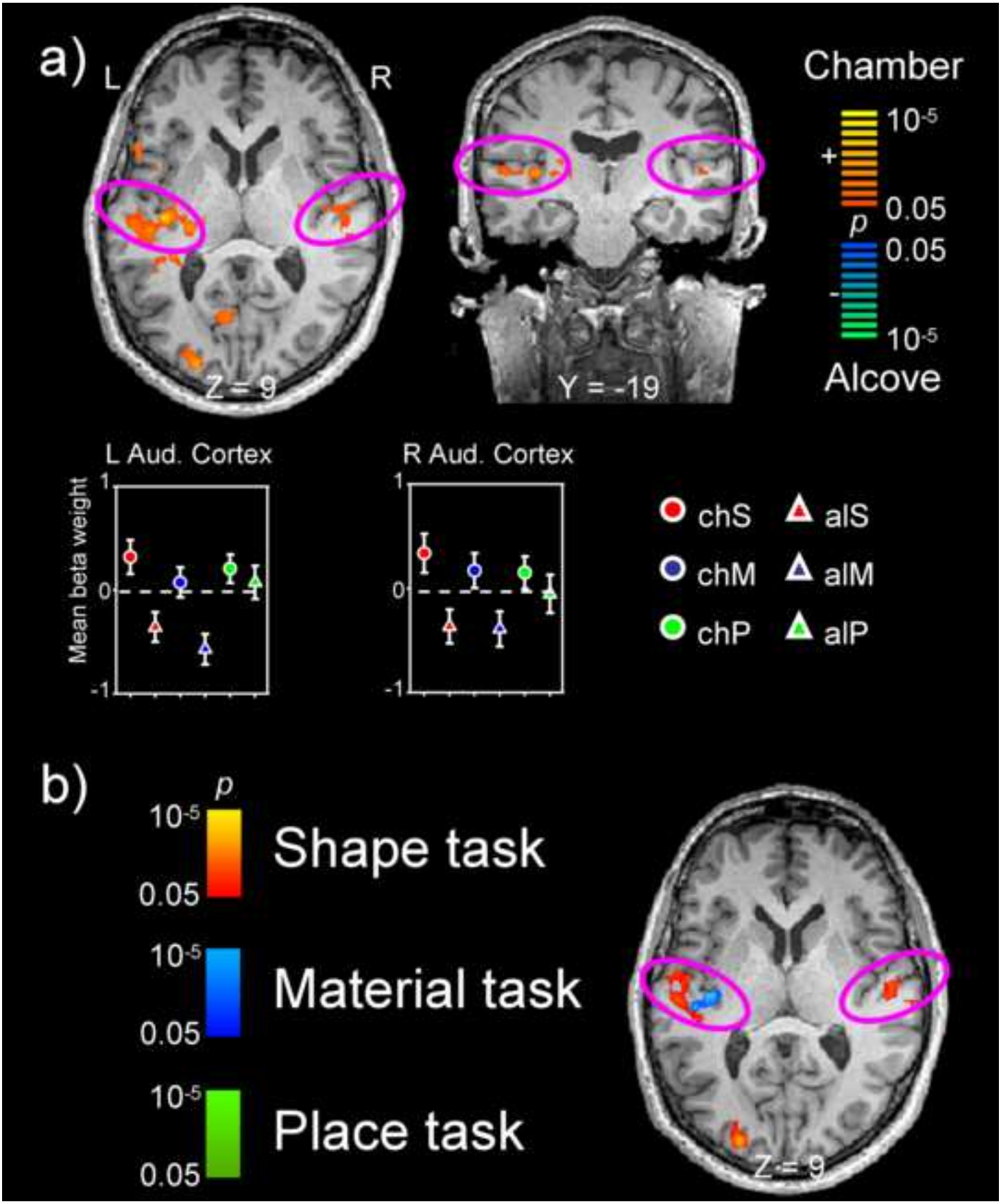

Figure 5

Click here to download high resolution image

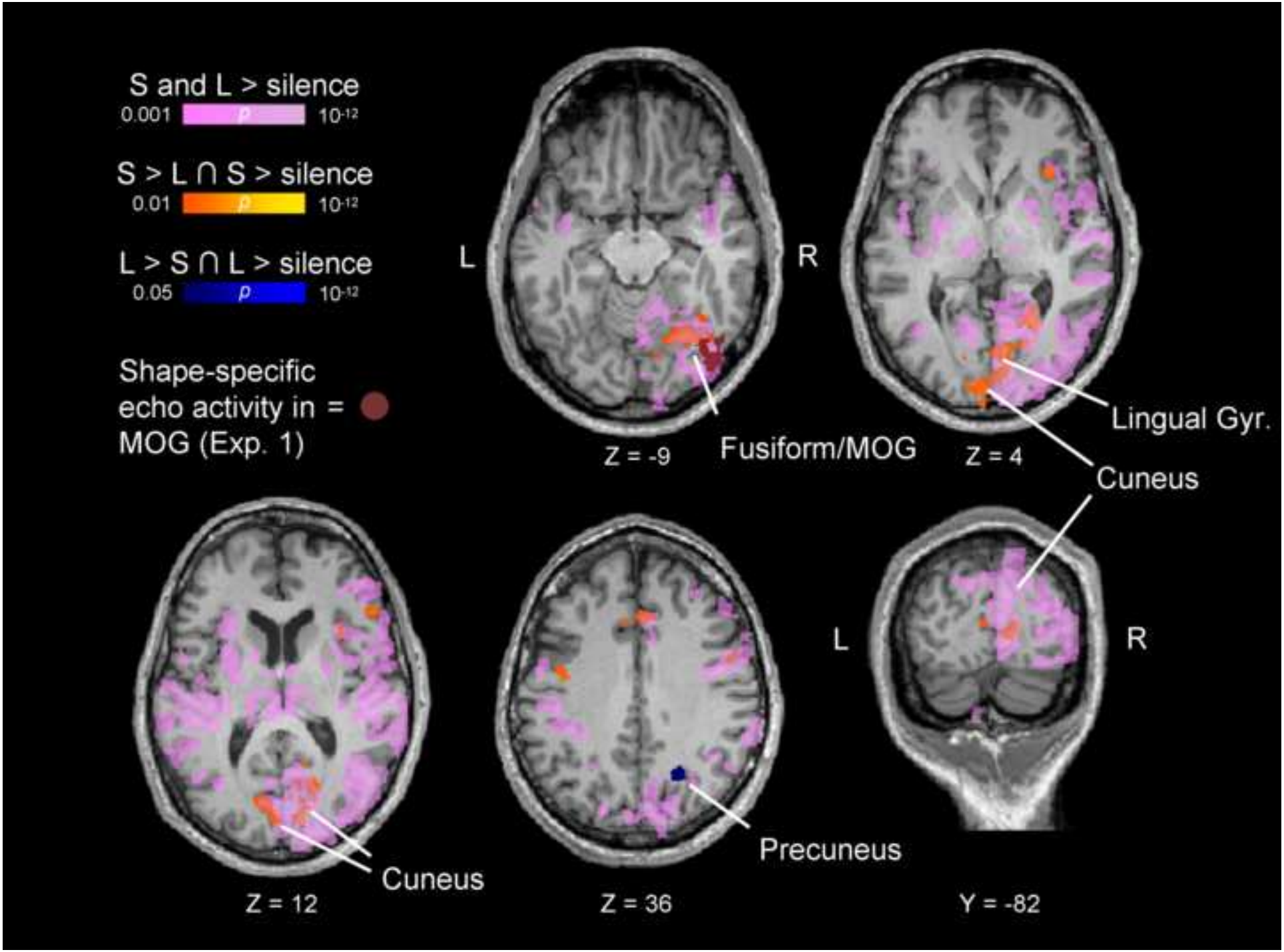

Figure 6

Click here to download high resolution image

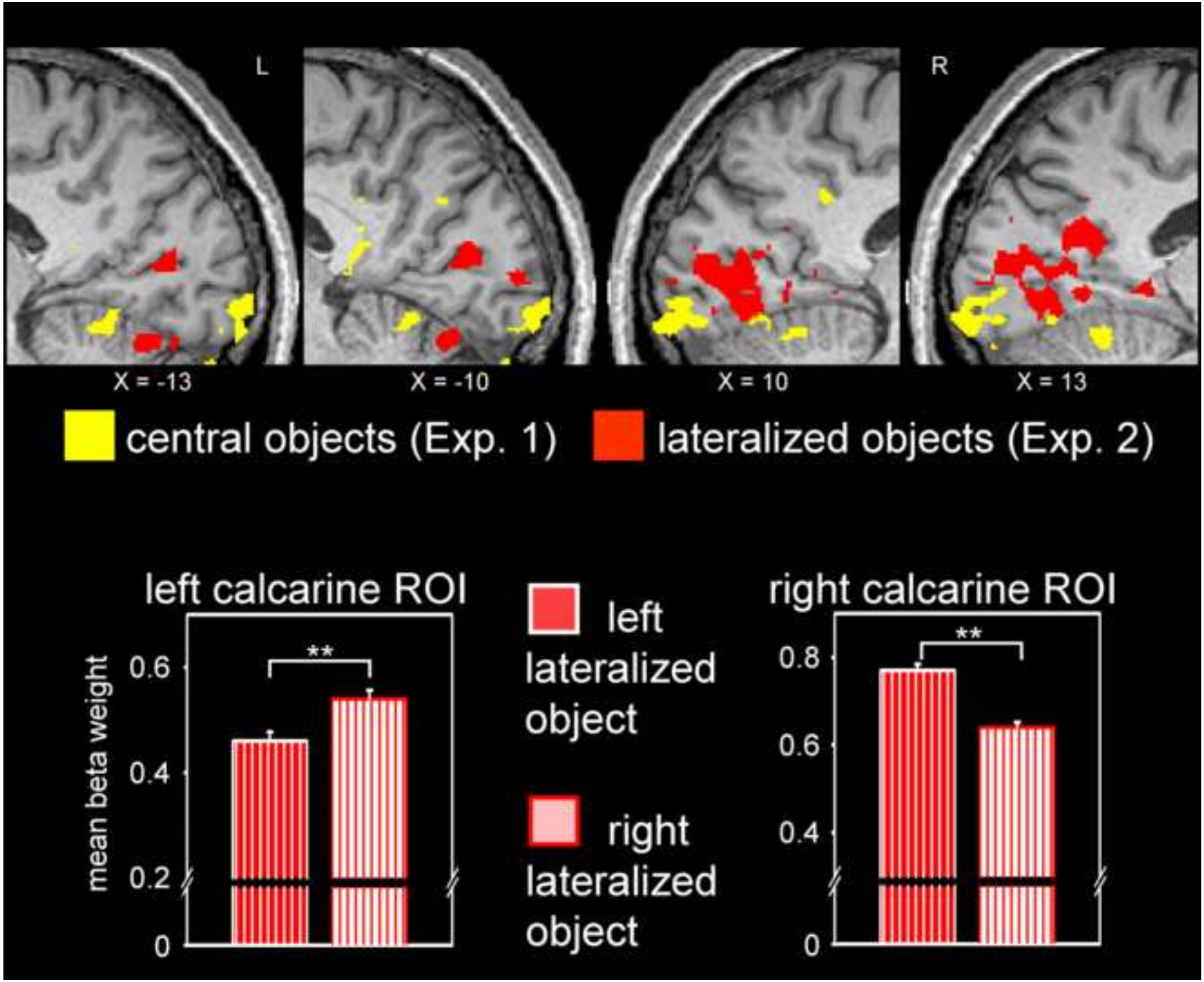

Supplementary Material

Click here to download Supplementary Material: Supplemental_Data_revisedNSY-D-12-00475.doc